Self-Association of the Polyene Antibiotic Nystatin in Dipalmitoylphosphatidylcholine Vesicles: A Time-Resolved Fluorescence Study

A. Coutinho*‡ and M. Prieto*

*Centro de Química-Física Molecular, Complexo I, Instituto Superior Técnico, 1096 Lisboa Codex and ‡Departamento de Química e Bioquímica, Faculdade de Ciências da U.L., 1700 Lisboa, Portugal

ABSTRACT The interaction between Nystatin and small unilamellar vesicles of 1,2-dipalmitoyl-*sn*-glycero-3-phosphocholine, both in gel (T = 21°C) and in liquid-crystalline (T = 45°C) phases, was studied by steady-state and time-resolved fluorescence measurements by taking advantage of the intrinsic tetraene fluorophore present in this antibiotic. It was shown that Nystatin aggregates in aqueous solution with a critical concentration of 3 μM. The enhancement in the fluorescence intensity of the antibiotic was applied to study the membrane binding of Nystatin, and it was shown that the antibiotic had an almost fivefold higher partition coefficient for the vesicles in a gel ($P = (1.4 \pm 0.1) \times 10^3$) than in a liquid-crystalline phase ($P = (2.9 \pm 0.1) \times 10^2$). Moreover, a time-resolved fluorescence study was used to examine Nystatin aggregation in the membrane. The emission decay kinetics of Nystatin was described by three and two exponentials in the lipid membrane at 21°C and 45°C, respectively. Nystatin mean fluorescence lifetime is concentration-dependent in gel phase lipids, increasing steeply from 11 to 33 ns at an antibiotic concentration of 5–6 μM, but the fluorescence decay parameters of Nystatin were unvarying with the antibiotic concentration in fluid lipids. These results provide evidence for the formation of strongly fluorescent antibiotic aggregates in gel-phase membrane, an interpretation that is at variance with a previous study. However, no antibiotic self-association was detected in a liquid-crystalline lipid bilayer within the antibiotic concentration range studied (0–14 μM).

INTRODUCTION

The polyene macrolide antibiotics are a group of compounds that share a common antifungal activity (Kobayashi and Medoff, 1977). Among their components, Amphotericin B (AmpB) and Nystatin have a special importance because they have been used in the treatment of systemic and superficial mycotic infections, respectively, in spite of the severe secondary effects that they exert (Medoff et al., 1983). These two antibiotics are closely related inasmuch as they have very similar molecular structures (Fig. 1), their major differences being their polyenic chains (whereas AmpB has a heptaene, the Nystatin molecule contains a tetraene plus a diene) and some configurations in the polyol region.

The polyene antibiotics act at the cell membrane level, where they increase the cell permeability to ions and small molecules, thereby promoting a leakage of important cellular constituents and ultimately lysis and death of the cell (Bolard, 1986). In several experiments (e.g., De Kruijff et al., 1974), the presence of sterols in the membranes was found to be an essential requisite for maximal polyene antibiotic sensitivity. Moreover, the antibiotic selectivity may be related to the type of sterol present in the plasmatic membrane; ergosterol-rich fungal membranes are much more sensitive to the action of the antibiotic than cholesterol-rich membranes, whereas sterol-free bacterial cells are quite resistant to these molecules (Kinsky et al., 1966). However, despite a large array of information obtained by a variety of techniques, there is still considerable controversy concerning the role of sterols in this process (for a comprehensive review see Bolard, 1986).

The most widely accepted model for the mode of action of these antibiotics assumes that they form aqueous pores in lipid membranes (Holz and Finkelstein, 1970). In fact, Ermishkin et al. (1976) succeeded in measuring single ionic channels in black-film membranes made from brain phospholipids. The formation of transmembrane pores constituted by antibiotic-sterol complexes, composed of alternated antibiotic and sterol molecules, was first proposed by De Kruijff and Demel (De Kruijff and Demel, 1974; Van Hoogevest and De Kruijff, 1978). On the other hand, Finkelstein and co-workers (Marty and Finkelstein, 1975; Kleinberg and Finkelstein, 1984) suggested that these antibiotics self-associated into pores and that sterols had only an ordering function in packing the polyene molecules together. HsuChen and Feingold (1973) had also previously proposed an indirect role for sterols in the mode of action of the antibiotics through their modulation of membrane organization, i.e., through their capacity to change the phospholipid packing in the membranes. According to these authors, the interaction between polyenes and membranes required the lipid bilayer to be in an ordered state. More recently, Bolard et al. (1991) suggested that the permeability pathways induced by AmpB or Nystatin in the membranes

Received for publication 12 May 1995 and in final form 15 September 1995.

Address reprint requests to Dr. Manuel J. Estevez Prieto, Centro de Química-Física Molecular, Instituto Superior Técnico, Av. Rovisco Pais, 1096 Lisboa Codex, Portugal. Tel.: 351-1-8419219; Fax: 351-1-3524372; E-mail: qmprieto@alfa.ist.utl.pt.

0006-3495/95/12/2541/17 $2.00

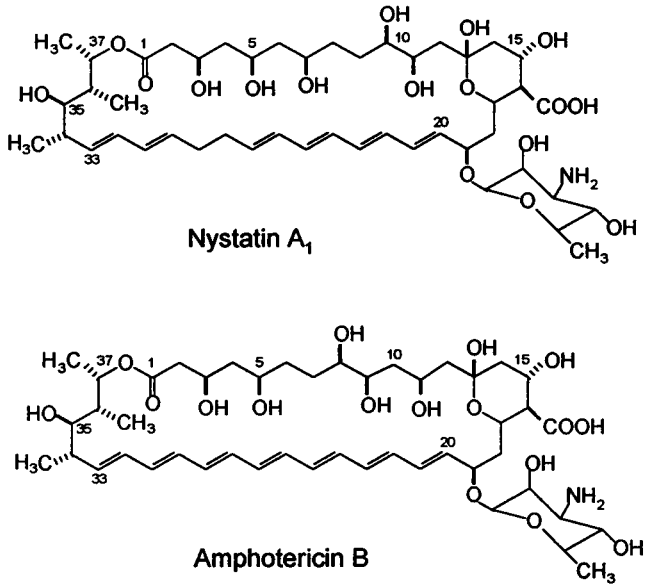

FIGURE 1 Molecular structures of Nystatin A_1 and Amphotericin B.

might depend on the type of sterol present in it. The formation of an antibiotic-sterol complex would still be a valid model for ergosterol-containing membranes, whereas for cholesterol-rich membranes the antibiotics had to be added to the aqueous solution in the self-associated form to be active. Later studies gave further support to this model (Legrand et al., 1992; Lambing et al., 1993). However, it was shown in a recent circular dichroism (CD) study (Balakrishnan and Easwaran, 1993a) that AmpB was capable of undergoing a concentration-dependent aggregation when incorporated into bilayer membrane systems without sterols. Moreover, these authors showed that ergosterol promoted drug aggregation, i.e., made it occur at a lower drug concentration. A completely different hypothesis for the mechanism of action of these compounds was put forward by Hartsel et al. (1991). These authors proposed that AmpB could be active at membranes without sterols through the formation of ion-conducting membrane defects at the antibiotic-lipid interface.

This work was focused on Nystatin, a polyene antibiotic that has been less frequently studied than AmpB. We have taken advantage of the intrinsic fluorescence properties of the tetraene chromophore present in this molecule to study its interaction with phospholipid bilayer membranes. Previous studies carried out with *trans*-parinaric acid (*t*-PnA) (Hudson and Cavalier, 1988), a fatty acid with the same fluorescent group as Nystatin, have shown that the tetraene is an excellent reporter of the properties of its microenvironment, namely of its close density. We expected that the fluorescence of Nystatin would also display this same sensitivity, which would eventually allow us to monitor different antibiotic species in the bilayer. Before addressing the role of sterols in the Nystatin mode of action, we have chosen to carry out this study with a simple model membrane system, namely sonicated vesicles prepared with 1,2-dipalmitoyl-*sn*-glycero-3-phosphocholine (DPPC) both in gel and in liquid-crystalline phases. The fluorescence properties of Nystatin were used here to characterize the partitioning of this antibiotic to the membrane and to examine its state of aggregation. Our results confirmed that the presence of sterols in the lipid bilayer is not essential for antibiotic binding to the vesicles and showed that Nystatin associates preferentially with gel-like over fluid-like lipids. Moreover, the changes in the emission decay kinetics of Nystatin clearly indicated a cooperative self-association of the membrane-bound antibiotic in gel-phase lipids.

EXPERIMENTAL PROCEDURES

Materials

Nystatin (pharmaceutical grade) was a gift from Squibb Farmacêutica Portuguesa through the courtesy of Dr. Horácio Santana, and it was stored at −20°C with exclusion of light. All other chemicals were obtained from commercial suppliers and were used without further purification. DPPC was purchased from Avanti Polar Lipids (Birmingham, AL)) and acetic acid, Tris(hydroxymethyl)aminomethane, NaCl, NaOH, HCl, and EDTA were obtained from Merck (Darmstadt, Germany). Methanol was spectroscopic or gradient grade and was purchased from Merck. A stock solution of Nystatin (~1 mM) was prepared in methanol and stored at −20°C. Nystatin concentration was determined by ultraviolet (UV) absorption ($\epsilon_{304\ nm} = 7.4 \times 10^4\ M^{-1}\ cm^{-1}$ in methanol).

Analysis and purification of Nystatin

Thin-layer chromatography (TLC) of Nystatin was performed on precoated silica gel plates (silica gel 60 TLC plates; Merck) according to Thomas et al. (1981). Briefly, the eluent consisted of the lower phase of chloroform-methanol-water (20:22:10, v/v/v). The plates were pre-run in the mobile phase and were then dried at 100°C for 30 min before use. After development in the dark, the plates were air dried and visualized either with UV light or by exposure to iodine vapors. The spots detected were scraped and the compounds were eluted from the silica with methanol. After a centrifugation step, these samples were subjected to gradient elution high-performance liquid chromatography (HPLC).

HPLC of Nystatin was performed on a Merck apparatus, which included a L-6200A pump, a L-5025 column chamber in conjunction with a L-4500 photodiode UV array detector. The separations were performed on a LiChrospher 100 RP-18 column (5 μm, 4 mm ID × 25 cm; Merck) with an identical pre-column (5 μm, 4 mm ID × 0.4 cm) at a flow rate of 0.7 ml/min, at 35°C. The solvent composition for all gradient runs was adapted from Thomas et al. (1981) and changed linearly from 60:40 methanol-5 mM sodium acetate (pH 5.8) buffer to 85:15 over a 30-min interval. Then it was maintained at that composition for an additional period of 10 min, and 40 min after injection the solvent composition was returned to 60:40. The purity was calculated as the percentage peak area corresponding to Nystatin divided by peak areas of total number of peaks in each chromatogram. For the semipreparative work, a 10 μm, 10 mm ID × 25 cm column also packed with LiChrospher 100 RP-18 was employed. The flow rate was 4 ml/min, and the effluents were manually fractionated and analyzed by analytical HPLC in the previously described conditions.

The fast atom bombardment (FAB) mass spectra were obtained with a Kratos MS-25RF instrument with the sample dispersed in a 3-nitrobenzyl alcohol matrix.

Model membrane preparation

Small unilamellar vesicles (SUVs) were prepared by sonication. Briefly, the dry lipid was dissolved in chloroform in a round-bottom flask and the

solvent was first dried under a stream of N_2 and then further evaporated under vacuum for at least 5 h. The dried lipid was dispersed to the desired concentration (1–5 mM) by adding the appropriate volume of 50 mM Tris-HCl (pH 7.4) buffer with 10 mM NaCl and 0.2 mM EDTA and by repeated vortexing at 50°C, well above the gel-to-liquid crystalline phase transition temperature (T_c) of the lipid. The resulting multilamellar dispersion was then sonicated until near-optical clarity using a Branson 250 sonicator with a standard flat tip. This process was interrupted periodically for 1 min to prevent overheating of the solution. The total sonication time was usually 30 min. After equilibration of the suspension at 50°C for 1 h (for the "annealing" process (Lawaczeck et al., 1976) to take place), the titanium particles released from the tip were removed by centrifugation at 10,000 × g for 15 min, at room temperature. The final lipid concentration of the solution was determined by phosphorus analysis (McClare, 1971). The sonicated vesicles were stored at room temperature if they were kept overnight before use.

Absorption and steady-state fluorescence measurements

Absorption spectra were measured at room temperature using a Jasco V-560 spectrophotometer. Fluorescence intensities were measured with a Spex F112A Fluorog spectrofluorometer with a double emission monochromator and a thermostatted cuvette holder (±1°C) using 0.5 cm pathlength quartz cuvettes. Unless otherwise stated, fluorescence intensities were measured at 315 nm excitation and 415 nm emission wavelengths with spectral bandwidths of 0.9 nm and 9.0 nm, respectively. These conditions were chosen to minimize Nystatin photochemical degradation during the fluorescence measurements. Stray light was reduced using a UV bandpass filter SB-300 (Corion) in the exciting beam and a WG-360 (Corion) cut-off filter in the emission beam, except in steady-state anisotropy measurements. Moreover, background intensities in Nystatin-free samples due to the vesicles were subtracted from each recording of fluorescence intensity. All the fluorescence measurements were carried out in a right-angle geometry, and the geometry effect (Parker, 1968) was taken into account when necessary. Correction of excitation and emission spectra were performed using a rhodamine B quantum counter solution and a standard lamp (Lackowicz, 1983), respectively.

The steady-state anisotropy, $\langle r \rangle$, defined by the relationship (Lackowicz, 1983)

$$\langle r \rangle = \frac{I_{VV} - GI_{VH}}{I_{VV} + 2GI_{VH}} \tag{1}$$

was obtained by measuring the vertical and horizontal components of the fluorescence emission with excitation vertical (I_{VV} and I_{VH}, respectively) and horizontal (I_{HV} and I_{HH}, respectively) to the emission axis. The G factor ($G = I_{HV}/I_{HH}$) corrects for the transmissivity bias introduced by the detection system. These measurements were made with Glan-Thompson polarizers, and background intensities due to the lipid vesicles were always taken into account.

Time-resolved fluorescence measurements

Fluorescence lifetimes were determined by the time-correlated single-photon timing technique. The instrument (Farinha et al., 1994) uses a nitrogen-filled flashlamp (Edinburgh Instruments, 119F) operated at 80 kHz as the excitation source. The excitation and emission wavelengths (316 nm and 415 nm, respectively) were selected with Jobin-Yvon H-20 monochromators with typical bandwidths of 4 and 8 nm, respectively. To avoid artefacts caused by stray light, a UG-11 (Newport) filter and a WG-360 (Corion) filter were placed in the excitation and emission beams, respectively. The emission light was detected at 90° by a Phillips XP2254B cooled (−30°C) photomultiplier to reduce background noise. Decay curves were collected into 1024 channels with 0.268 or 0.122 ns/channel resolution, and 10^4 counts were accumulated in the peak channel. Data collection was carried out using a solution of 1,4-bis(5-phenyl-1,3-oxazol-2-yl)benzene in cyclohexane as a reference (τ = 1.1 ns; Lampert et al., 1983), and the δ-function convolution method (Zuker et al., 1985) was applied in data analysis.

Fluorescence intensity decay curves were analyzed by nonlinear least-squares regression, fitting the data to a sum of exponentials as expressed by Eq. 2:

$$I(t) = \sum_{i=1}^{n} \alpha_i e^{-t/\tau_i} \tag{2}$$

where α_i and τ_i are the normalized amplitude ($\Sigma_i \alpha_i = 1$) and lifetime of the ith decay component, respectively. The reduced χ^2 value and weighted residuals with their autocorrelation were used as best-fit criteria. The range of χ^2 values obtained was 1.0–1.3.

The mean lifetime, $\langle \tau \rangle$, is defined by Eq. 3:

$$\langle \tau \rangle = \frac{\sum_{i=1}^{n} \alpha_i \tau_i^2}{\sum_{i=1}^{n} \alpha_i \tau_i} \tag{3}$$

and the fractional intensity, f_i, of the ith decay component is given by

$$f_i = \frac{\alpha_i \tau_i}{\sum_{i=1}^{n} \alpha_i \tau_i} \tag{4}$$

Partitioning of Nystatin into the vesicles

The interaction of a compound with phospholipid vesicles is usually followed by adding a liposome stock solution successively to an aqueous solution of the molecule in study. After each addition, a spectroscopic signal of the bound compound is measured to monitor the interaction. However, the high susceptibility of Nystatin to photochemical degradation, characteristic of compounds with tetraene chromophores (Morgan et al., 1980), prevented us from following this methodology. Instead, several dilutions of a stock solution of SUVs (~5 mM) with buffer were prepared. Then, a constant volume from the Nystatin stock solution was injected into each of these samples. The final volume of methanol in solution never exceeded 1.5% of the total volume of each sample. After an incubation time of 1 h in the dark and at room temperature, the fluorescence intensity of each sample was measured as a function of the lipid/antibiotic ratio in the conditions previously described (see Absorption and Steady-state Fluorescence Measurements, above). The partitioning experiments were carried out at 21 ± 1°C and 45 ± 1°C, and the data were analyzed according to Eq. 5 (see Appendix):

$$\Delta I = \frac{\Delta I_{max}[L]}{1/(P\gamma) + [L]} \tag{5}$$

In this equation, $\Delta I = I - I_0$ stands for the difference between the fluorescence intensity of the antibiotic measured in the presence (I) and in the absence of phospholipid vesicles (I_0); $\Delta I_{mean} = \Delta I_\infty - I_0$ is the maximum value of this difference, because I_∞ is the limiting value of I measured upon increasing the lipid concentration, $[L]$, of the solution; P is the partition coefficient of the antibiotic between the aqueous and lipid phases and γ is the molar volume of the lipid. As the partitioning experiments were carried out with SUVs, it was considered that only 60% of the overall lipid used was available for the initial partition of the antibiotic (Beschiaschvili and Seelig, 1990); this is equivalent to the fraction of lipid present in the outer leaflet of the bilayer. The molar volumes of DPPC in SUVs in the gel (γ = 0.828 dm^3mol^{-1}) and liquid-crystalline (γ = 0.949 dm^3mol^{-1}) phases were estimated as described in Castanho et al. (1995).

RESULTS

Characterization of Nystatin complex

Nystatin is an antibiotic produced by *Streptomyces noursei*, which is known to be a complex mixture of closely related compounds (Kleinberg and Finkelstein, 1984). The composition of Nystatin includes at least three tetraene antibiotics, namely Nystatin A_1 (which is considered to be the main component of pharmaceutical-grade Nystatin), A_2, and A_3 (Zielinski et al., 1988). Kleinberg and Finkelstein (1984) showed that the minor tetraene components present in their Squibb Nystatin samples (accounting for nearly 20% of the mixture) did not present any activity in their assays with asolectin/ergosterol (2.5:1) membranes. The presence of a small heptaene contaminant in Nystatin complex has also been reported (Kleinberg and Finkelstein, 1984). These two classes of polyene antibiotics are easily distinguished via their absorption spectra, because the tetraene typically shows absorption maxima in ethanol at 292, 305, and 320 nm, whereas the heptaene absorption maxima are at 364, 383, and 408 nm (Petersen, 1985).

The partial separation of the Nystatin complex was achieved by HPLC (Fig. 2). The chromatogram shows the presence of one major tetraene component (peak 1) and two unresolved lesser components (peak 2). Based on the measurement of peak areas, the main component comprised 82.0%, whereas the second peak accounted for 16.3% of the total area. Moreover, two small heptaene impurities could be separated from the Nystatin complex (peaks 3 and 4). From the absorption spectra of Nystatin, these heptaene contaminants were estimated to be approximately 2 mol% if a molar absorptivity equivalent to AmpB was used (Petersen, 1985).

The FAB mass spectra of Nystatin complex showed molecular ions at *m/z* 948 $[M + Na]^+$, 926 $[M + H]^+$, and 908 $[(M + H) - H_2O]^+$. Because these peaks are close to those expected for Nystatin A_1, this must be the major component of the complex used (peak 1 of Fig. 2).

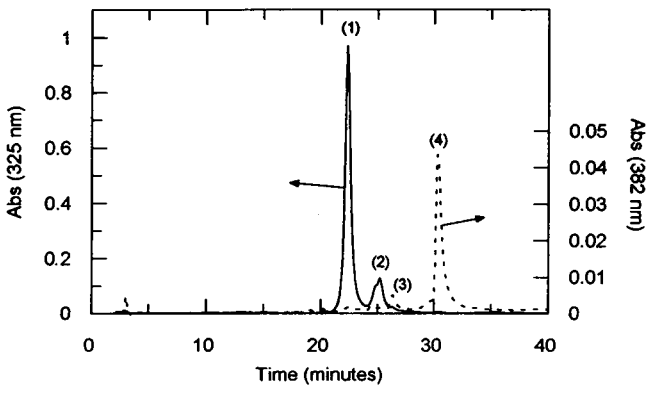

FIGURE 2 Separation of Nystatin complex by gradient HPLC. A Li-Chrospher RP-18 column was eluted at a flow rate of 0.7 ml/min, at 35°C with a 30-min duration linear solvent gradient starting from an initial 60% A/40% B and ending with a 85% A/15% B solvent mixture (solvent A, methanol; solvent B, 5 mM sodium acetate (pH 5.8) buffer). The final solvent mixture was run for 10 min, and 40 min after injection the solvent composition was returned to 60:40. Peaks (1), and (2), tetraene components; peaks (3), and (4), heptaene components.

The heptaenes and some minor tetraene contaminants could be successfully separated from the main tetraene components of Nystatin by TLC. However, a posterior analysis by HPLC of the partially purified samples showed that the ratio between the two main tetraene peaks 1 and 2 decreased relative to the parent complex. This unexpected result, which implied an enrichment of the sample by the components present in peak 2, could be explained by a preferential retention of the main component of Nystatin by the silica. A similar result had already been described for another polyene antibiotic, Filipin (Kelly and Nabinger, 1985). Because we were interested in the opposite effect, we did not proceed with this technique.

A semipreparative purification of Nystatin by HPLC was also tried, but the complete elimination of peak 2 was not achieved. These partially purified Nystatin samples were used later in the time-resolved fluorescence experiments and gave results (decay components) identical to the ones obtained with the parent mixture.

These observations, together with the fact that all of the major components of the Nystatin complex are tetraenes (i.e., they have identical absorption properties) and that the heptaenes are nonfluorescent molecules (Petersen and Henshaw, 1981), prompted us to use the Nystatin complex in the subsequent experiments.

Self-association of Nystatin in buffer and in methanol

Solutions of Nystatin in 50 mM Tris-HCl (pH 7.4) buffer with 10 mM NaCl and 0.2 mM EDTA were prepared from dilution of a stock solution of Nystatin in methanol. To detect the possible aggregation of the antibiotic, its fluorescence intensity and steady-state anisotropy were measured as a function of antibiotic concentration in buffered solution (Fig. 3). It should be noted that the precision of the anisotropy measurements was low because of the negligibly small quantum yield of Nystatin in aqueous solution ($\phi < 0.003$; Castanho et al., 1992). At low concentrations of Nystatin, the anisotropy increased with the concentration of antibiotic in solution; however, above ~3 μM antibiotic the anisotropy reached a maximum of 0.28 $\pm$ 0.03 and became concentration-independent. At this antibiotic concentration, there was also a sharp increase in the fluorescence intensity of Nystatin. These observations are consistent with an aggregation of the antibiotic in aqueous solution, a process that was previously described (Castanho et al., 1992). In this former study, it was also shown that the self-association of the antibiotic in solution was accompanied by an increase in the vibrational resolution of its emission spectra and in the light-scattering intensity of the solution.

The same study was repeated in methanol (results not shown). In this solvent, Nystatin fluorescence intensity

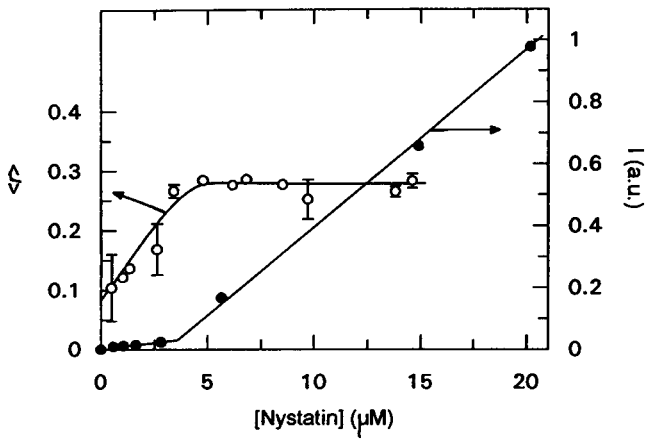

FIGURE 3 Variation of the steady-state fluorescence anisotropy, $\langle r \rangle$ (○) and fluorescence intensity, I (●) (λ_{exc} = 304 nm; λ_{em} = 410 nm) with Nystatin concentration in 50 mM Tris-HCl (pH 7.4) buffered solution with 10 mM NaCl and 0.2 mM EDTA.

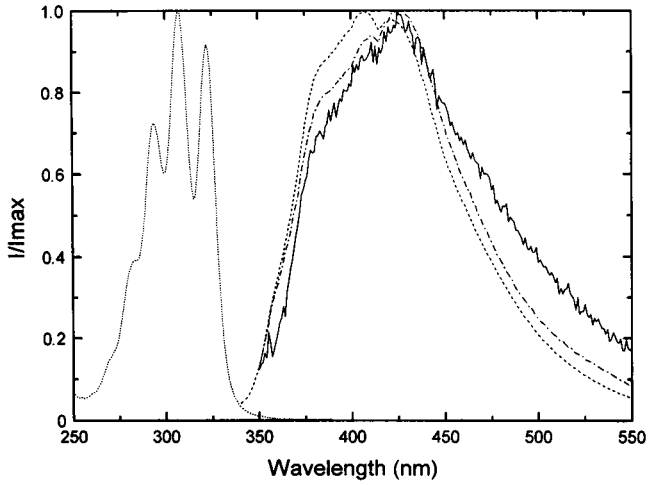

FIGURE 4 Normalized and corrected fluorescence spectra of 6.5 μM Nystatin. ····, Excitation spectra in the presence of 3 mM SUVs of DPPC, at 21°C (λ_{em} = 415 nm). ——, Emission spectra in buffer (50 mM Tris-HCl, pH 7.4, with 10 mM NaCl and 0.2 mM EDTA) and in the presence of 3 mM SUVs of DPPC prepared with the same buffer at 21°C (– – –) and at 45°C (– · –) (λ_{exc} = 315 nm).

showed a linear dependence with concentration (0–25 μM). On the other hand, the light-scattering intensity of the solution was nearly constant within this concentration range of antibiotic, showing a steep increase only for Nystatin concentrations larger than 100–200 μM (results not shown). These results indicate that the antibiotic is virtually monomeric in methanol until it reaches this high concentration in solution.

Fluorescence spectra of Nystatin

To gain insight into the interaction between Nystatin and the phospholipid bilayer vesicles of DPPC, we investigated the changes in the fluorescence properties of the antibiotic in the presence of SUVs. Fig. 4 shows the normalized and corrected emission spectrum of 6.5 μM Nystatin in buffer and its normalized and corrected excitation and emission spectra in the presence of 3 mM small unilamellar vesicles of DPPC, at 21°C and 45°C. The excitation spectrum of self-associated Nystatin in aqueous solution presents three maxima at 293 nm, 306 nm, and 321 nm and a shoulder at 282 nm (not shown in Fig. 4 for the sake of clarity). Upon the addition of phospholipid vesicles in gel (T = 21°C) or liquid-crystalline phases (T = 45°C) to this solution, this spectrum underwent a redshift of 1 nm, and it was found to be essentially independent of the temperature of the sample. On the other hand, the emission spectrum of Nystatin at 21°C was less broad and gained spectral resolution when compared to the one obtained for Nystatin in buffer. Furthermore, the fluorescence intensity of Nystatin was greatly enhanced, as shown by the higher signal-to-noise ratio of the first spectrum relative to the second one. In contrast, a much less pronounced increase in Nystatin fluorescence intensity could be observed upon its interaction with the lipid vesicles above the gel-to-liquid-crystalline phase transition temperature of DPPC (T_c = 41°C) (see also Fig. 5). At 45°C, the wavelength of maximum fluorescence intensity of Nystatin underwent a redshift relative to 21°C (from 408 to 426 nm), and the Nystatin emission spectrum lost vibrational resolution, presenting now a closer resemblance with the spectrum obtained for Nystatin in aqueous solution. Altogether these results indicate that Nystatin interacts with the phospholipid vesicles at both temperatures. Moreover, no alterations were observed either in the excitation or in the emission spectra of Nystatin as a function of antibiotic concentration in the presence of the lipid vesicles, at both temperatures.

Nystatin binding to the lipid vesicles

The increase in the fluorescence intensity of Nystatin associated with the interaction between the antibiotic and the lipid vesicles was used to measure its partition into SUVs of DPPC, both in gel and in liquid-crystalline phases. Fig. 5 shows the enhancement in Nystatin fluorescence for samples in which the antibiotic concentration was kept constant while the lipid concentration was varied. This study could not be carried out using high concentrations of Nystatin and lipid, because of the detected fusion/aggregation of the vesicles induced by the binding of the antibiotic. This process was noticed by the increase in the baseline of the absorption spectra of the antibiotic in the presence of the lipid vesicles relative to a control turbidity spectrum measured with an antibiotic-free lipid solution. This increase was particularly pronounced when the lipid vesicles were in the gel phase and for antibiotic concentrations greater than approximately 9 μM. In those conditions, the presence of larger light-scattering particles in solution reduced the transmitted light and thus caused the fluorescence intensity of Nystatin to decrease suddenly when the ratio of lipid to antibiotic in solution was increased. Therefore, low concen-

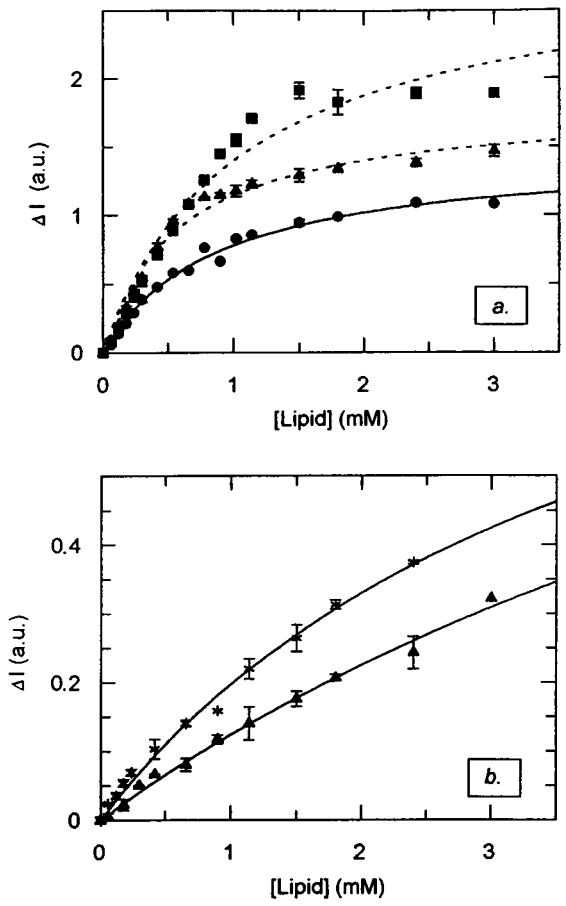

FIGURE 5 Enhancement of the fluorescence intensity of Nystatin upon increasing the lipid concentration in solution (SUVs of DPPC) (*a*) at 21°C and (*b*) at 45°C. The Nystatin concentrations used were (●) 4.2 μM, (▲) 6.5 μM, (■) 7.8 μM, and (*) 13.5 μM. [Lipid], accessible lipid concentration = 60% of total lipid concentration. Error bars represent the standard deviation of duplicate or triplicate measurements at the indicated lipid concentration. The full curves are nonlinear least-squares fittings of Eq. 5 to the data points, which were used to yield estimates of the partition coefficients, *P*. The dashed curves are displayed just to show the poorer fittings obtained for these two antibiotic concentrations.

trations of Nystatin were used in this study at 21°C. According to the model proposed (see Appendix), the fluorescence intensity data obtained for 4.2 μM Nystatin at 21°C (Fig. 5 *a*) were fitted to Eq. 5 to yield estimates of ΔI_{max} and *P*. The partition coefficient thus obtained was $(1.4 \pm 0.1) \times 10^3$. The same procedure was also followed with the data obtained for 6.5 and 7.8 μM antibiotic, but a hyperbolic curve, as the one predicted by Eq. 5, could not adequately describe the experimental results, as judged by the poorer fits obtained in these cases (Fig. 5 *a*). It should be noted, especially for 7.8 μM antibiotic, that the increase in its fluorescence intensity leveled off toward a plateau almost abruptly at a lipid concentration around 1.5 mM. This result suggests that some antibiotic was being retained in the aqueous phase even if the lipid phase was further extended, indicating that for these antibiotic concentrations a more complex model than the one presented in the Appendix is needed to describe the partitioning of the antibiotic into the lipid vesicles.

The partitioning study of Nystatin was also carried out with the phospholipid vesicles above T_c. At 45°C, the scattering artifacts caused by the vesicles were less critical and higher Nystatin concentrations could be used. At this temperature, the binding curves were far from reaching a plateau within the lipid concentration range accessible to this experimental study (Fig. 5 *b*). This result indicates that the interaction between the antibiotic and the phospholipid vesicles was weaker in the liquid-crystalline phase; in fact, a lower partition constant of $(2.9 \pm 1.0) \times 10^2$ was estimated for Nystatin by the fitting procedure previously described.

Steady-state fluorescence anisotropy measurements

The steady-state fluorescence anisotropy of Nystatin as a function of total lipid concentration in solution is plotted in Fig. 6 *a*. These measurements were performed either by adding several aliquots of 5 mM SUVs of DPPC to aqueous solutions of Nystatin or by direct injection of a Nystatin stock solution into the lipid vesicles. Therefore, the final concentrations of both antibiotic and lipid were varyied for each series of measurements. At 21°C, the limiting anisotropy of Nystatin for diluted solutions of small unilamellar vesicles of DPPC was estimated to be 0.33 ± 0.01, and it was found to be independent of the lipid-antibiotic ratio used. However, as the concentration of the lipid was increased above approximately 2 mM, a gradual decrease in the steady-state anisotropy of Nystatin was measured (Fig. 6 *a*). For a set of samples in which the concentration of the lipid was kept constant and the final Nystatin concentration in solution varied (Fig. 6 *b*), the anisotropy of the antibiotic was found to be independent of the lipid-antibiotic ratio used, although it progressively decreased for each set of samples prepared with a higher lipid concentration (results not shown).

These measurements were harder to perform at 45°C because of the decrease in the fluorescence intensity of the antibiotic at this temperature (see Fig. 5). Therefore, it was possible to obtain reproducible values only for total lipid concentrations greater than 2.5 mM. Again, the anisotropy of Nystatin was found to be independent of the lipid-antibiotic ratio used, and a constant value of 0.31 ± 0.03 was measured for its limiting anisotropy (results not shown).

Time-resolved fluorescence measurements

Gel phase

The fluorescence intensity decay curves measured for 3.0 and 12.5 μM Nystatin in the presence of 3 mM sonicated vesicles of DPPC at 21°C are shown in Fig. 7. As judged from the fitting criteria (χ^2 value and random weighted residuals and autocorrelation plots), the experimental data

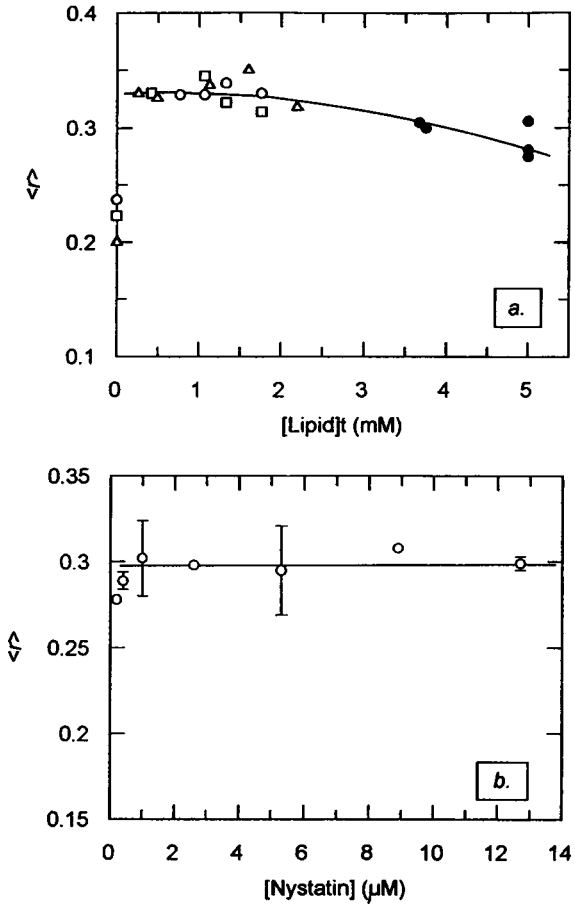

FIGURE 6 Variation with (*a*) total lipid concentration and (*b*) antibiotic concentration in solution of the steady-state fluorescence anisotropy, $\langle r \rangle$, of Nystatin in SUVs of DPPC at 21°C. (*a*) The samples were prepared by titrating (□) 7.1 μM, (△) 14.2 μM, or (○) 21.3 μM antibiotic aqueous solution with 5 mM SUVs of DPPC or (●) by direct injection of the antibiotic stock solution to the lipid vesicles. The antibiotic concentration varied from 4.9 to 14.6 μM in this last case. (*b*) [Lipid]t = 1 mM.

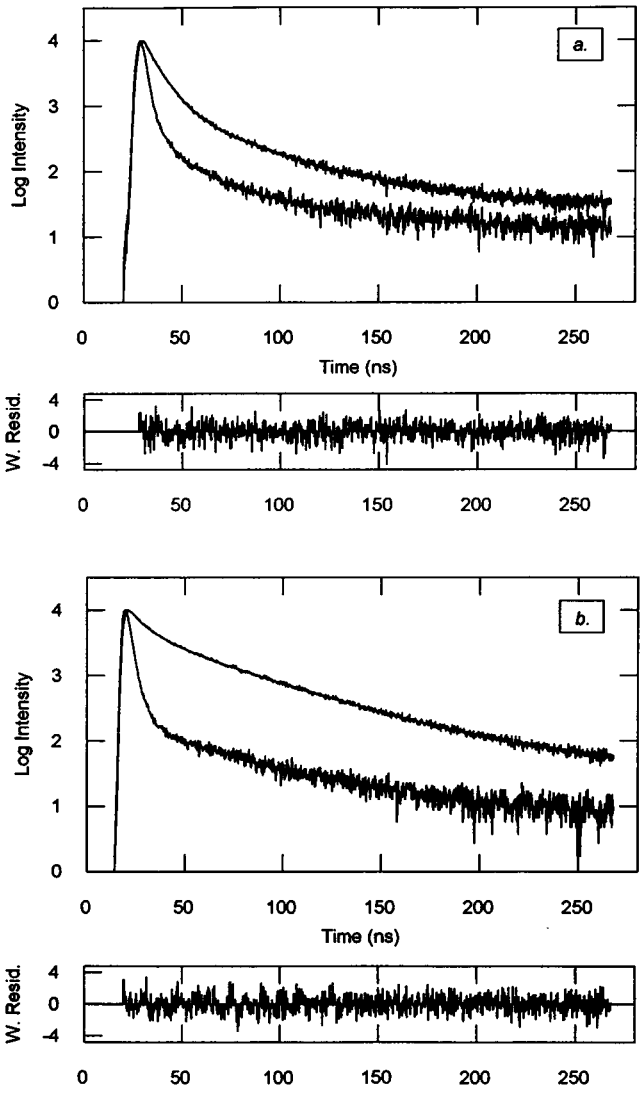

FIGURE 7 Time-resolved fluorescence intensity of (*a*) 3.0 μM and (*b*) 12.5 μM Nystatin in the presence of 3 mM SUVs of DPPC, at 21°C (λ_{exc} = 316 nm; λ_{em} = 415 nm). Both the fluorescence response of 1,4-bis(5-phenyl-1,3-oxazol-2-yl)benzene and the experimental and calculated patterns of the antibiotic are shown (1024 channels; time resolution, 0.268 ns/channel). The three-component fits to the data were: (*a*) α_1 = 0.56; τ_1 = 1.7 ns; α_2 = 0.41; τ_2 = 7.1 ns; α_3 = 0.03; τ_3 = 34.1 ns; χ^2 = 1.099; and (*b*) α_1 = 0.50; τ_1 = 2.4 ns; α_2 = 0.29; τ_2 = 10.2 ns; α_3 = 0.21; τ_3 = 38.3 ns; χ^2 = 1.194. The goodness of fit is demonstrated by the weighted residuals plots.

could be described by a sum of three exponentials (Table 1). These curves also show a concentration dependence for the emission decay kinetics of Nystatin upon its interaction with lipid vesicles in a solid-like gel phase because 12.5 μM antibiotic (Fig. 7 *b*) displays a longer-lived mean fluorescence lifetime than 3.0 μM (Fig. 7 *a*) (30.0 and 11.7 ns, respectively). To further characterize this dependence, several fluorescence decay curves were obtained with different Nystatin final concentrations (solutions prepared with a fixed lipid concentration of 3 mM). Fig. 8 shows the fluorescence decay parameters of Nystatin recovered from one set of those experiments. Several features of these values are noteworthy. Upon increasing Nystatin concentration in solution, there was a sharp increase in the amplitude of the longest-lived decay component (α_3), from approximately 0.03 to 0.25, at an antibiotic concentration of about 5–6 μM (Fig. 8 *a*). An opposite change occurred with the normalized pre-exponential associated with the intermediate lifetime (α_2), which decreased sharply from nearly 0.40 to 0.28 in the same antibiotic concentration range. On the other hand, the amplitude associated with the shortest lifetime (α_1) showed a gradual decrease in its value from about 0.58 to 0.46. Concomitantly with these alterations, both the longest and intermediate lifetimes (τ_3 and τ_2, respectively) increased slightly with Nystatin concentration, whereas the shortest lifetime (τ_1) remained essentially concentration independent (Fig. 8 *b*). As a consequence of these changes, the intensity-weighted mean lifetime of Nystatin (Fig. 8 *c*) displayed an almost steplike enhancement from nearly 11 to 33 ns at an antibiotic concentration of approximately 5–6 μM. This increase resulted primarily from the contribution

TABLE 1 Fluorescence intensity decay parameters of Nystatin in small unilamellar vesicles of 3 mM DPPC as a function of Nystatin concentration and temperature

T (°C)	[Nystatin][§] (μM)	α_1	τ_1 (ns)	α_2	τ_2 (ns)	α_3	τ_3 (ns)
21*	3.0 (8)	0.55	2.4	0.41	8	0.03	33
	10.5 (3)	0.55	2.9	0.24	14	0.21	42
	12.5 (4)	0.50	2.4	0.30	11	0.21	37
45‡	2.3–16.0[¶] (7)	0.75	1.2	0.25	4.2		

α_i and τ_i are the average values of the normalized amplitude and lifetime, respectively, of each decay component, for n decay measurements.
* α_1, ±0.04; τ_1, ±0.7; α_2, ±0.05; τ_2, ±3; α_3, ±0.05; τ_3, ±5 ns.
‡ α_1, ±0.02; τ_1, ±0.1; α_2, ±0.02; τ_2, ±0.2 ns.
§ The values in parenthesis indicate the number, n, of measurements.
¶ The decay components were independent of Nystatin concentration.

of the longest lifetime component, whose fractional intensity (calculated from Eq. 4) increased from approximately 0.17 to 0.63.

Because the precision associated with the decay parameters of Nystatin was low (see Table 1), a study of the reproducibility of the change in the emission decay kinetics of Nystatin was carried out. Fig. 9 shows that the sharp transition measured for the Nystatin mean fluorescence lifetime always occurred within a narrow range of antibiotic concentrations (between 5 and 7 μM). Moreover, the partially purified Nystatin samples by HPLC also exhibited the same trend of variation in their decay parameters upon varying the antibiotic concentration in solution. The addition of Nystatin methanolic solution to the suspension of vesicles at 45°C instead of 21°C (i.e., above the phase transition temperature of DPPC) also had no influence on Nystatin fluorescence intensity decays measured subsequently at 21°C.

These results indicate that the tetraene fluorophore of Nystatin is experiencing a different environment in the lipid bilayer as its total concentration in solution exceeds 5–6 μM. Furthermore, the critical behavior shown by the decay parameters of Nystatin suggests that a cooperative transition is taking place, which is only compatible with the antibiotic undergoing a self-association in the membrane. Strong evidence for the presence of Nystatin aggregates in the lipid vesicles was provided by a simple experiment. This consisted of submitting a sample of lipid vesicles with preincorporated antibiotic to a brief sonication pulse. The fluorescence intensity decay of Nystatin was measured prior to and after this treatment, and conversion of the slow decaying to the fast decaying species was observed, suggesting that the sonication pulse disrupted the aggregates of Nystatin. The possibility of Nystatin degradation during this experiment was ruled out by performing a careful fluorescence characterization of the sample before and after this procedure.

Two additional experiments were carried out to obtain more information about the formation of these strongly fluorescent antibiotic aggregates. First, a sample of lipid vesicles pre-incubated with Nystatin (13.7 μM) and exhibiting a typical long mean lifetime was diluted with buffer to an antibiotic final concentration of 4.6 μM. After a short incubation period, the emission decay kinetics of Nystatin

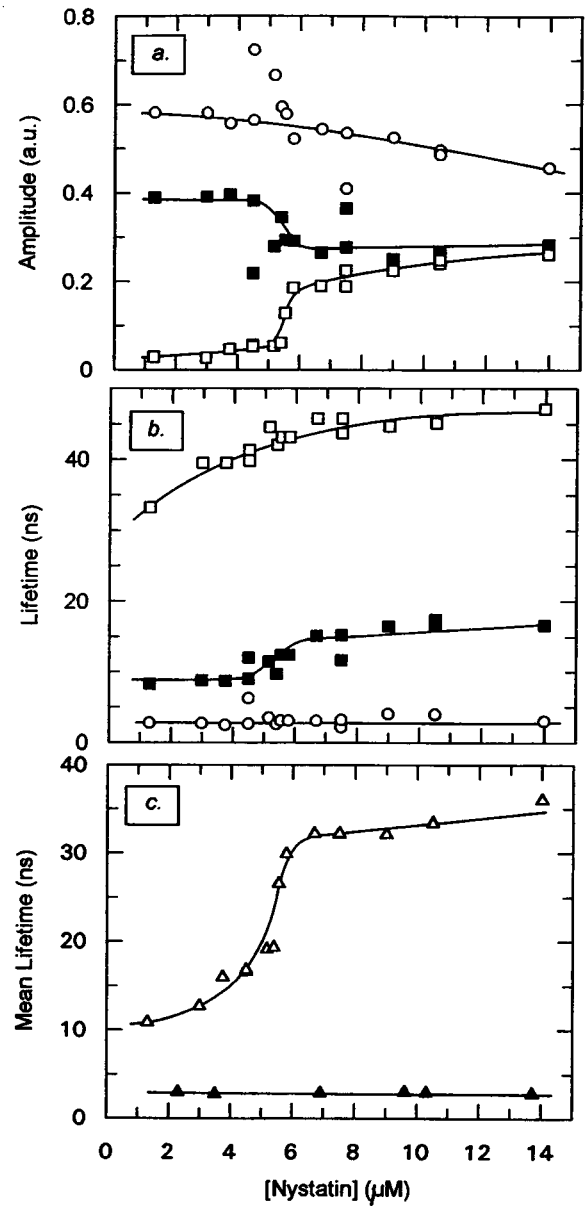

FIGURE 8 The concentration dependence of the fluorescence decay parameters of Nystatin in 3 mM SUVs of DPPC. (*a*) Normalized amplitudes, α_i and (*b*) fluorescence lifetimes, τ_i of the (○) short-, (■) intermediate-, and (□) long-lived decay components of Nystatin at 21°C, respectively. (*c*) Mean excited-state lifetime, $\langle\tau\rangle$ ($\langle\tau\rangle = \sum_i \alpha_i\tau_i^2/\sum_i \alpha_i\tau_i$) of the antibiotic, at (△) 21°C and (▲) 45°C.

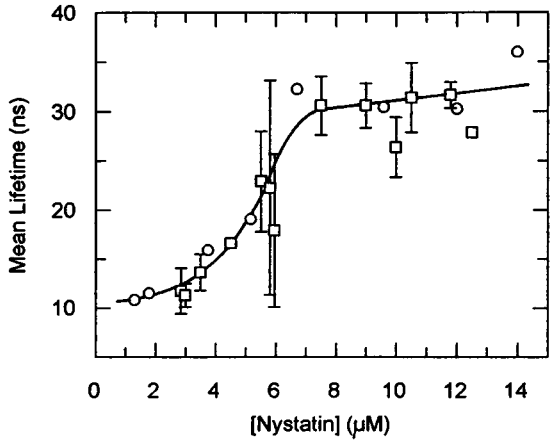

FIGURE 9 The concentration dependence of the mean excited-state lifetime, $\langle\tau\rangle$ (see the legend of Fig. 8) of Nystatin in 3 mM SUVs of DPPC, at 21°C. ○, single measurements; □, the error bars represent the standard deviation of at least duplicate measurements at the indicated antibiotic concentration.

was found to remain constant. However, if the dilution procedure was repeated using SUVs (at the same initial lipid concentration) instead of buffer, the fluorescence intensity decay of Nystatin changed into one characteristic of a 4.6 μM sample. These results suggest that the removal of Nystatin from the membrane to the aqueous phase follows a slow kinetics. On the other hand, the exchange of antibiotic molecules between the lipid vesicles must be a very fast and predominantly intervesicular process, causing the dissociation of the aggregates.

Liquid-crystalline phase

Results of a three-component and two-component analysis of the fluorescence intensity decays of 9.6 μM Nystatin in 3 mM DPPC bilayers are shown in Fig. 10 as a function of temperature. Above the DPPC phase transition temperature, no contribution from the longest lifetime component to the fluorescence decay could be detected (Fig. 10 *a*), and the fluorescence decays of the antibiotic were now satisfactorily fitted by a biexponential instead of a three-exponential function, as revealed by the low χ^2 values obtained and by the random distribution of the weighted residuals (results not shown). The abrupt variations observed in the pre-exponential factors of the shortest and intermediate-lifetime components at T_c are a consequence of this change in the analysis function of the emission decay kinetics of the antibiotic (Fig. 10 *a*). Both the intermediate and longest-lived lifetime components could detect the phospholipid thermotropic phase transition temperature, as evidenced by the steep change in their magnitude at ~41°C (Fig. 10 *b*). In contrast, the shortest lifetime component of the fluorescence decay of Nystatin was almost temperature independent (Fig. 10 *b*) and did not sense this transition.

The fluorescence decay parameters obtained for a final antibiotic concentration in solution lower than the critical

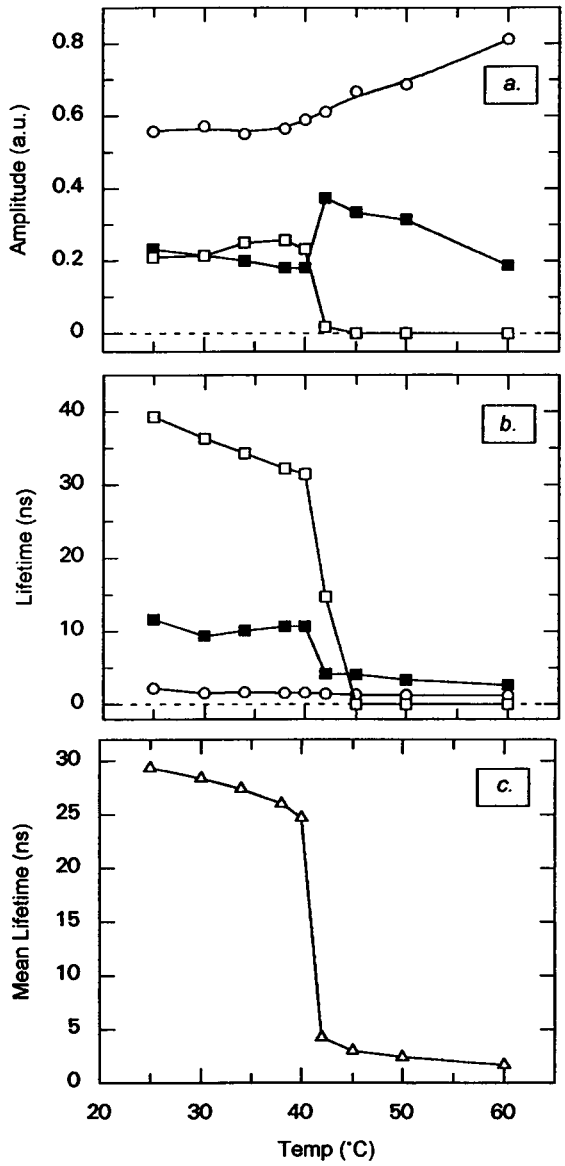

FIGURE 10 Variation with temperature of the fluorescence decay parameters of 9.6 μM Nystatin in 3 mM SUVs of DPPC. (*a*) Normalized amplitudes, α_i; (*b*) fluorescence lifetimes, τ_i of the (○) short-, (■) intermediate-, and (□) long-lived decay components, respectively; (*c*) △, mean excited-state lifetime, $\langle\tau\rangle$ (see the legend of Fig. 8) of Nystatin. It should be noted that above 41°C the fluorescence decays were fitted to a two-exponential function.

concentration range previously described (5–7 μM) showed a similar temperature dependence. Furthermore, the decay parameters of Nystatin were found to be concentration independent at 45°C within the concentration range studied (0–14 μM) (Fig. 8 and Table 1).

DISCUSSION

Characterization of Nystatin complex

The structure of Nystatin A_1, the main component of Nystatin complex, has been elucidated (Borowski et al.,

1971) (Fig. 1), and it was shown to contain a glycosidally linked mycosamine at C-19. Another constituent of Nystatin complex, Nystatin A_3, contains digitoxose as an additional neutral sugar at C-35 (Zielinski et al., 1988). No information could be found relative to Nystatin A_2 except that it has a molecular ion $[M + H]^+$ with a *m/z* value lower than that of Nystatin A_1 (910 and 926, respectively (Mitrofanova et al., 1991)). Because this component has the same sugar but it is less polar than Nystatin A_1 (Manwaring et al., 1969), we conclude that their chemical structures must differ in the number of hydroxyl groups present in the lactone ring.

The aim of this study was to perform a photophysical characterization of Nystatin to obtain structural information on its interaction with model membranes, and so it was important to guarantee the purity of the antibiotic samples used. The gradient HPLC analysis showed that all of the major components of this antibiotic complex were tetraenes and that the heptaene contaminants accounted for only 2 mol% of the sample. Because these last compounds are nonfluorescent (Petersen and Henshaw, 1981), its small content in the antibiotic complex should not interfere with our measurements. Another potential problem related to the use of nonpurified antibiotic is the presence in the sample of molecules with the same fluorophore but which establish distinct interactions with the lipid bilayers, e.g., Nystatin A_1 and A_3, because of their different chemical structures. Although the only structural difference between these two compounds is the additional digitoxose in Nystatin A_3, this second sugar moiety may produce different membrane locations and therefore cause distinct photophysical behaviors for these two antibiotic molecules. However, the molecular ion of Nystatin A_3 (*m/z* 1056 $[M + H]^+$ (Zielinski et al. (1988)) was not detected in the FAB mass spectra of Nystatin complex and hence it must be present in a very small amount in our samples, if at all. After certifying that the partially purified Nystatin samples by HPLC and the parent mixture had identical photophysical properties in lipid bilayers, this study was then safely carried out with the Nystatin complex.

The aggregation of Nystatin in homogeneous media

The fluorescence intensity data (Fig. 3) clearly showed that Nystatin at concentrations higher than 3 μM is forming aggregates in aqueous solution that have a larger quantum yield than monomeric antibiotic, in agreement with what was reported in a preliminary study (Castanho et al., 1992). The steady-state fluorescence anisotropy of Nystatin confirmed this conclusion, since its increase is further evidence for the formation of larger antibiotic species in solution as the antibiotic concentration was raised. This reasoning is based on the expectation that the lifetime of the aggregate must be longer than the one of the monomer because of the measured increase in its quantum yield. The fluorescence lifetime of Nystatin in aqueous solution could not be measured accurately because of the time resolution of our instrumentation, an upper limit of approximately 100 ps being reported in the literature (Petersen et al., 1987). This experimental difficulty also prevented us from estimating the volume of the aggregate by application of the Perrin and Stokes-Einstein equations in a simple approximation (spherical geometry; Lackowicz, 1983) to the steady-state anisotropy data. Nevertheless, if we admit that the fluorescence lifetime of the aggregate is independent of Nystatin concentration in solution, the constant value measured for its steady-state anisotropy above 3 μM suggests that it has also a constant correlational time or, in other words, a constant volume. Accordingly, the anisotropy data are consistent with a micellization-type equilibrium of the antibiotic in aqueous solution with a critical concentration of approximately 3 μM.

In methanol, the fluorescence intensity data showed that the molecule exists as a monomer in solution, irrespective of its concentration within the range studied (0–25 μM). The formation of oligomers, detected by the increase in the light-scattering intensity of the solution, was only noticeable for antibiotic concentrations larger than 100 μM.

The chemical structures of Nystatin and AmpB show a close resemblance, both molecules having a hydrophobic side with their polyene chains, and a hydrophilic side with several polar substituents (Fig. 1). Besides this lateral asymmetry, which confers on these molecules their amphiphilic character, most of their hydroxyl groups are positioned axially on the same side of the plane of the lactone ring, together with the mycosamine moiety. These characteristics make the antibiotics very poorly water soluble and only moderately soluble in organic solvents. The formation of aggregates of polyene antibiotics in different solvents had previously been studied by several techniques, namely electronic absorption, circular dichroism, light scattering, and nuclear magnetic resonance (Rinnert et al., 1977; Mazerski et al., 1990; Balakrishnan and Easwaran, 1993b). The aggregation behavior found for Nystatin is in agreement with the former studies carried out with AmpB, which showed that this last antibiotic exists monomerically only in polar organic solvents (methanol, ethanol, dimethylformamide, and dimethylsulfoxide). In particular, for a phosphate buffered saline (pH = 7.4) solution, a CD study of Nystatin showed that this antibiotic self-associated at a critical concentration of 10 μM (Bolard et al., 1991). Considering that this study was carried out at a different temperature (37°C) and that this process is strongly dependent on the temperature, among other factors (Bolard et al., 1991), there is a reasonable agreement between the two results.

Fluorescence spectral alterations of Nystatin

The blueshift undergone by the fluorescence emission spectra of Nystatin upon adding lipid vesicles to the solution, at either 21°C or 45°C (Fig. 4), demonstrated unequivocally that the antibiotic molecules interacted with the lipid bilay-

ers at either temperature and that their fluorophores were experiencing a less polar environment. This effect was more pronounced for the vesicles in a gel phase because concomitantly to this shift the emission spectrum of the antibiotic also increased its vibrational structure. These changes are also compatible with the inclusion of the chromophore in a more rigid environment because this behavior had previously been detected upon the formation of large antibiotic aggregates in the aqueous phase (Castanho et al., 1992) and upon decreasing the temperature of an ethanolic solution of Nystatin to 77 K (Bel'kov and Bondarev, 1987). Curiously, the emission spectrum of Nystatin in fluid-like phospholipid vesicles displayed a close similarity to its aqueous fluorescence emission, except that it was less broad.

The spectroscopic properties of Nystatin may be compared with those of *t*-PnA, a naturally occurring 18-carbon fatty-acid which has also a conjugated all-*trans*-tetraene chromophore. It should be taken into consideration, however, that apart from their polyene chains these two molecules have very different chemical structures that may influence their absorption and fluorescence properties as well as the chromophore location in the lipid bilayer. Thus, 1) the fluorescent group of Nystatin is inserted into a lactone ring, which must introduce constraints on its mobility, and 2) this group is in close vicinity to a diene and to a glycosidic linkage (Fig. 1). Finally, 3) the tetraene chromophore of *t*-PnA is located near the terminal methyl group of its chain because *t*-PnA is a 9,11,13,15-all-*trans* fatty acid. It has also been recently shown (Castanho et al., 1995) that this group is located deep inside the bilayer, whether the membrane is in a gel or liquid-crystalline phase. On the other hand, the tetraene group of Nystatin is positioned near its mycosamine sugar, which is positively charged at the pH of our experiments (Mazerski et al., 1990). Hence, it is very unlikely that it has the same location as the chromophore of *t*-PnA in a bilayer. Most probably the antibiotic must be adsorbed at the bilayer surface or, if inserted vertically, its tetraene group must nevertheless be in close vicinity to the more polar region of the bilayer.

The absorption spectrum of *t*-PnA is blueshifted relative to the one of *cis*-parinaric acids (Sklar et al., 1977a). Interestingly, the absorption of Nystatin is identical to that obtained for the *cis* and not for the *trans* fatty-acid isomer. This is certainly due to the more complex structure of Nystatin, where its all-*trans* chromophore may be participating in through-bond interactions with the diene chain and adjacent oxygen, and therefore it may be stabilized. Another difference between Nystatin and *t*-PnA is the changes undergone by their excitation spectra upon varying the environment of their fluorescent chromophores. The excitation spectrum of *t*-PnA exhibits a blueshift on going from the higher density gel phase to the lower density liquid crystalline phase because of the increase of the medium polarizability (Sklar et al., 1977b). It was even reported (Hudson et al., 1986) that the environment of this probe can be characterized in terms of its density by determining its excitation maximum. Yet, the excitation spectrum of Nystatin remained unchanged upon increasing the temperature of the lipid vesicles above T_c. A possible explanation for this result is the expected difference in the location of the two chromophores in a lipid bilayer, as discussed above. The shallower location anticipated for the antibiotic chromophore in the lipid bilayer and its inclusion in a lactone ring must prevent the establishment of a close contact between it and the acyl chains of the surrounding phospholipids. Consequently, it does not sense a significant variation of the refractive index of its micro-environment upon varying the temperature of the system, which is at variance with what was observed with *t*-PnA. In spite of these differences between Nystatin and *t*-PnA, the equivalence between their photophysical properties is so large that it justifies the use of *t*-PnA as a model compound of Nystatin fluorescence properties, as we shall discuss later.

Partition of Nystatin between phospholipid and aqueous phases

The fluorescence enhancement of Nystatin was used to assess its binding to the phospholipid vesicles. Because the fluorescence intensity of Nystatin in aqueous solution is almost negligible but becomes considerable when the probe is included in a hydrophobic environment, this parameter is a sensitive reporter of its partition into the bilayer vesicles. The partition coefficients of Nystatin determined for small unilamellar vesicles of DPPC in gel (T = 21°C) and liquid-crystalline (T = 45°C) phases were $(1.4 \pm 0.1) \times 10^3$ and $(2.9 \pm 0.1) \times 10^2$, respectively. In spite of the low accuracy of this last value owing to the experimental difficulty in reaching a plateau in the fluorescence signal, these results clearly show that the antibiotic has a higher binding affinity for a more ordered, rigid-like lipid phase than for a fluid one. Previous binding studies carried out with Nystatin and AmpB and employing different techniques had also reached the same conclusion (Abramson and Ockman, 1973; Bolard et al., 1981; Jullien et al., 1988). It is worthwhile to note that regardless of their hydrophobicity, these polyene antibiotics do not partition into the lipid bilayers to a very large extent when added from the aqueous phase because of their ability to form water-soluble aggregates.

The results obtained in the partition study of 6.5 and 7.8 μM antibiotic at 21°C showed a poorer agreement between experimental data and the theoretical analysis derived in the Appendix. This model considers exclusively the existence of a single species in solution that may be incorporated into a bilayer membrane according to a partition equilibrium. However, we have previously shown that above a threshold of around 3 μM antibiotic, Nystatin self-associates in aqueous solution and so, for these two antibiotic concentrations, and particularly for 7.8 μM, aggregates of antibiotic must be also present in solution. Hence, this more complex situation, which includes at least an additional aggregation equilibrium in solution, is no longer adequately described by our partition model. At 45°C, the critical concentration

of Nystatin is shifted to a higher value (Bolard et al., 1991), and thus the simple partition model derived in the Appendix is now fulfilled in a wider Nystatin concentration range.

The fluorescence properties of Nystatin had already been the subject of a thorough study, both in homogeneous solution (Petersen, 1985) and phospholipid vesicles (Petersen et al., 1987). Although our experimental results show essentially a general agreement with those reported in those studies, our interpretation is totally different from theirs on several points. Petersen et al. (1987) reported that Nystatin is quenched in bilayer membranes by a static process, the quenching being equally efficient in both the gel and liquid-crystalline phases of the bilayer. The main experimental evidence presented in their study to support the existence of a static quenching process was that Nystatin quantum yield decreased while its average lifetime remained unchanged for samples in which the total concentration of Nystatin was kept constant and the phospholipid concentration was progressively decreased to a final 25-fold dilution. To explain these results, Petersen et al. (1987) tried to fit their data to a fluorescence resonance energy-transfer model (heterotransfer) in two dimensions (Snyder and Freire, 1982). We think that their reasoning is totally inconsistent because 1) this mechanism of quenching predicts a decrease in the fluorescence intensity as well as of the fluorescence lifetime of the donor, which is incompatible with the results reported by Petersen et al. 2) Energy migration (homotransfer), and not heterotransfer, is the only possible interaction in a system with only one component. This point will be discussed later in more detail. Finally, 3) Petersen et al. described the model applied as dynamic, but its derivation did not consider diffusional processes. Based in our previous discussion, we propose a different explanation for their results. As the phospholipid concentration in solution was decreased, a smaller fraction of the overall antibiotic present in each sample partitioned into the lipid phase. This implied a decrease in the quantum yield of the antibiotic because this parameter was evaluated relative to the overall antibiotic concentration in solution and not only relative to the fraction partitioned into the lipid bilayer. On the other hand, Nystatin fluorescence lifetime did not vary because this antibiotic is almost nonfluorescent in the aqueous phase. In fact, if we re-analyze the results of Petersen et al. (1987) presented in their table 3 according to our partition model (see the Appendix), we obtain a satisfactory fit, and a partition constant of 2.3×10^3 is estimated, admitting that both layers of the model system of membranes are accessible to the antibiotic incorporation. This result is in reasonable agreement with our own determinations, considering that different experimental conditions were used in each case, namely distinct model systems of membranes (small unilamellar vesicles prepared by sonication versus ethanol injection), phospholipids (DPPC versus 1, 2-dimyristoyl-*sn*-glycero-3-phosphocholine), and buffers (50 mM Tris-HCl, pH 7.4, with 10 mM NaCl and 0.2 mM EDTA versus phosphate-buffered saline, pH 7.4). Moreover, it should also be stressed that the increase in the quantum yield of a tetraene upon its binding to hydrophobic sites is a general property of this fluorophore. In fact, it had already been used extensively to study the binding of Lucensomycin, another tetraene-containing polyene antibiotic with a smaller (C_{25}) lactone ring, to erythrocyte ghosts (Strom et al., 1976), the binding of *t*-PnA to hydrophobic sites in proteins (Sklar et al., 1977c; Berde et al., 1979), and the partition of this fatty acid into lipid vesicles (Sklar, 1980).

The main conclusion of the study by Petersen et al. (1987) was that the fluorescence of Nystatin was quenched in a static process through the formation of antibiotic aggregates within the lipid bilayer. These were nonfluorescent, at variance with the monomeric antibiotic species. However, the demonstration of a static quenching process requires different experimental planning to discard aqueous/lipid partitioning effects. Thus, the samples should be prepared with the same amount of lipid and a varying Nystatin concentration to ensure a constant fraction of antibiotic in the membrane bilayer. By following this experimental procedure, we obtained a fluorescence signal linearly dependent on the total antibiotic concentration added to the lipid solution. Besides an irreversible photochemical dimerization reaction (Morgan et al., 1980), the only other report that we found in the literature of a self-quenching process for a derivative of *t*-PnA was a study by Somerharju et al. (1981). These authors synthesized a phospholipid containing a *cis*-parinaroyl moiety at the *sn*-2-position and found that lipid vesicles prepared exclusively with this probe displayed a very low fluorescence. The self-quenching process of this probe occurred with a 50% efficiency for vesicles containing approximately 10 mole% of labeled phosphatidylcholine (Somerharju et al., 1983). This value should be compared with the results of Petersen et al. (1987) (Fig. 3), which show an almost 100% quenching efficiency at a Nystatin-to-lipid ratio of only 0.02. In conclusion, we think that the explanation for the quenching of Nystatin quantum yield measured by these authors is a variable binding of the antibiotic to the lipid vesicles within the phospholipid concentration range used by Petersen et al. (1987), and not the formation of nonfluorescent Nystatin complexes.

Steady-state fluorescence anisotropy of Nystatin

The limiting anisotropies of Nystatin determined for infinite lipid dilution were $\langle r \rangle = 0.33 \pm 0.01$ and $\langle r \rangle = 0.31 \pm 0.03$ for SUVs of DPPC in solid-like gel and fluid-like liquid-crystalline phases, respectively, in agreement with a previous report (Petersen et al., 1987). In contrast, the steady-state fluorescence polarization of *t*-PnA showed a sharp decrease at the temperatures corresponding to phase changes in the lipid bilayer (Sklar et al., 1977b). Although the temperature dependences of the mean lifetimes of Nystatin and *t*-PnA are rather similar, at least for antibiotic concentrations larger than 6 μM (see next section), their anisotropy behaviors are quite distinct. This difference must be then related to the chemical structures of these two

compounds and eventually to their different locations in the lipid bilayer. Whereas Nystatin is a bulky molecule, *t*-PnA is a fluorescent probe with a structural similarity to the acyl chains of the phospholipids. Hence, the large size of Nystatin must prevent this molecule from reorienting its transition dipole in the bilayer during its excited-state lifetime, even when it is present in a more fluid environment such as a lipid bilayer in a liquid-crystalline phase.

Petersen et al. (1987) measured a decrease in Nystatin steady-state fluorescence anisotropy at high Nystatin densities in the bilayer vesicles. For this set of experiments, these authors used a constant phospholipid concentration while the Nystatin concentration was changed. We were not able to reproduce their results because the only way we succeeded in measuring a decrease in Nystatin anisotropy was by increasing the lipid concentration in solution (Fig. 6 *a*). In those conditions, it is well known that the source of the anisotropy decrease is artifacts caused by the scattering properties of the lipid vesicles (Lentz et al., 1979). Even admitting that the anisotropy measurements obtained by Petersen et al. are not hampered by this artifact, we think that their interpretation is again subject to strong criticism. These authors tried to explain their experimental results using now an energy-transfer model for homotransfer in two dimensions (Snyder and Freire, 1982). The only interaction that may cause a decrease in the fluorescence polarization of a fluorophore upon increasing its concentration is indeed energy migration (homotransfer). In fact, this experimental observation and an invariance of the fluorophore lifetime and steady-state fluorescence intensity with its concentration, are used as criteria to confirm the existence of this kind of interaction. But, more importantly, as with any other dipolar energy transfer process between a donor and an acceptor molecule, an essential requisite for its occurrence is the existence of a substantial spectral overlap between the emission and absorption spectra of the two molecules, respectively. This can hardly be the case with Nystatin, as can be judged from Fig. 3. Because of the specific photophysics of tetraenes (Hudson and Kholer, 1974), namely the fact that their absorption and emission properties are determined by transitions between different electronic states (absorption: $S_2 \leftarrow S_o$; emission: $S_1 \rightarrow S_0$), Nystatin absorption and emission spectra are clearly distinct and widely separated, showing almost no overlap between them. This implies that the Förster radius, R_o, for the Nystatin-Nystatin pair should be very low and certainly never be equal to 4.5 nm, the value recovered by Petersen et al. (1987) in their fitting of the energy migration model to the anisotropy data. Hence, energy migration must be a very inefficient process for Nystatin and cannot be the explanation for the decrease measured by Petersen et al. (1987) for the anisotropy of this antibiotic. Beyond a bias introduced in their measurements due to an increased light-scattering of the solution (e.g., caused by a variation in the lipid vesicles properties, namely their size, induced by an increased content of Nystatin in the bilayer), we do not envisage other hypothesis to explain their experimental results.

Self-association of Nystatin in lipid vesicles

Before proceeding with the discussion, some photophysical properties of *t*-PnA will be briefly reviewed because they are a determining factor in the interpretation of our experimental results. It has now been unequivocally shown using the maximum entropy method that even in homogeneous solution (like ethanol, cyclohexane, and paraffin oil) *t*-PnA displays a complex emission decay kinetics described by a bimodal fluorescence lifetime distribution (Mateo et al., 1993). This same pattern is followed by this probe in lipid bilayers well above their thermotropic transition temperature. However, near this temperature and below, a third lifetime component centered at higher values appears that was interpreted as corresponding to the emission of the probe localized in the gel phase (Mateo et al., 1993). Therefore, the fluorescence kinetics of this fatty acid is extremely sensitive to changes in the density of its close environment. Results similar to these had previously been found by using different methods of fluorescence decay analysis that considered either a sum of discrete lifetimes (Ruggiero and Hudson, 1989) or an a priori defined lifetime distribution (James et al., 1987).

The changes measured in the fluorescence intensity decay kinetics of Nystatin with temperature, when the antibiotic was partitioned into SUVs of DPPC, displayed the same pattern as previously described for *t*-PnA. In particular, the abrupt variation undergone by the antibiotic mean lifetime with the temperature (Fig. 10 *c*) reported accurately the thermotropic transition temperature of DPPC obtained for large unilamellar and multilamellar vesicles ($T_c = 41.4 \pm 0.5$°C; Marsh, 1990) and not the one expected for SUVs ($T_c \cong 38$°C; Harkness and White, 1979). This result provides then additional evidence for the fusion/aggregation of the lipid vesicles induced by the binding of Nystatin. It should also be noted that the longest-lived decay component of Nystatin did not persist at temperatures above T_c, which is at variance with what was observed with *t*-PnA.

An important finding of our study that to our knowledge had not been described before for a tetraene fluorophore is the concentration dependence shown by the emission decay kinetics of Nystatin in gel-phase lipids. Although the analysis of the fluorescence decay of the antibiotic in this lipid phase always required a long-lived component for the fit to converge to a low χ^2 value, it had a very small amplitude associated with it for Nystatin concentrations lower than 5–6 μM. Above this concentration, however, this normalized pre-exponential acquired a significant value and this increase could account almost by itself for the simultaneous change measured in the mean lifetime of the antibiotic (Fig. 8).

The observation that this variation in the emission decay kinetics of Nystatin took place upon increasing its concentration in solution raised the possibility that it could be associated with an extended perturbation of the bilayer properties because of an increased partitioning of the antibiotic into the lipid vesicles. The association of a foreign

molecule to a gel-like lipid bilayer is anticipated to occur in a local defect, probably contributing to the disorganization of the phospholipids surrounding the molecule. Therefore, if this hypothesis were correct, a decrease in the normalized amplitude of the long-lived decay component of Nystatin upon increasing the overall antibiotic concentration in solution would be expected, and not the opposite effect. Another possibility is that this photophysical behavior of Nystatin could be associated with the fusion/aggregation of the vesicles. However, this hypothesis is contradicted by the step-like dependence measured for the antibiotic mean lifetime with its concentration, because a monotonous increase would then be predicted. Moreover, preliminary experiments carried out with large unilamellar vesicles (Coutinho and Prieto, manuscript in preparation), where the fusion/aggregation of the vesicles induced by the antibiotic is not significant, gave a similar dependence of the mean lifetime on the antibiotic concentration in solution, although with a smoother variation.

By combining the above considerations of the photophysics of *t*-PnA with our present results, it can then be concluded that Nystatin is sensing a more rigid environment, i.e., it is experiencing a more restricted mobility, upon increasing its total concentration. To explain this observation, it is necessary to assume that at least two antibiotic species coexist in the bilayer. These could be distinct states of aggregation of the antibiotic in the bilayer because the self-association of Nystatin could decrease the nonradiative rate constant of this molecule and, consequently, cause an increase in its mean lifetime. In fact, it has been reported that the sensitivity of *t*-PnA lifetime to the environment is due primarily to variations in its nonradiative rate constant (Sklar et al., 1977a). Therefore, by assuming that the radiative rate constant and molar absorptivity of each antibiotic species in the bilayer are the same and considering only a two-states model for the sake of simplicity, the molar fraction of antibiotic with the longest mean lifetime, X_L, may be estimated from its normalized fluorescence amplitude, i.e., $X_L = \alpha_3$. This same procedure has been previously used to compute the fraction of *t*-PnA in bilayer regions with different lateral densities (Mateo et al., 1991, 1993).

The concentration dependence of α_3, and consequently of X_L, displayed in Fig. 8 *a* shows a cooperative character, confirming that the antibiotic is self-associating. The sonication experiment gives additional support to this conclusion. Two possible explanations can then be put forward to explain this result. First, different antibiotic species, e.g., monomers and aggregates pre-assembled in the aqueous phase, could be partitioning between the aqueous and lipid phases. On the other hand, Nystatin self-association could be a process restricted to monomeric antibiotic molecules already in interaction with the lipid bilayer. The first hypothesis, however, does not seem plausible because 1) it would require that the aggregates of antibiotic exhibited the same molecular arrangements in very different environments. Yet, inverted molecular organizations, i.e., with the antibiotic polar groups oriented toward the outside and toward the inside of the aggregate in the aqueous and lipid phases, respectively, are a more likely picture. Also, 2) the critical concentration measured for the aggregation process in the membrane (~6 μM) does not coincide with the value obtained in aqueous solution (3 μM). And finally, 3) the dilution experiment with antibiotic-free lipid vesicles provided evidence for the rapid redistribution of antibiotic molecules between the lipid vesicles, in agreement with was previously shown to occur with AmpB (Bolard et al., 1981). Furthermore, this experiment suggests that the main factor controlling the formation of the long-lived Nystatin species is the antibiotic-to-lipid ratio used. An important point that should be stressed is that the aggregation model discussed above does not exclude the possibility that simultaneously with its self-association, Nystatin may be also undergoing a change in its location in the lipid vesicles, e.g., moving from the surface of the membrane to the interior of the bilayer. This issue will be addressed in a later paper (Coutinho and Prieto, manuscript in preparation).

The fluorescence decay parameters displayed by Nystatin deserve a further comment. These values exhibit a close similarity with those published for *t*-PnA (Mateo et al., 1993), only for concentrations larger than ~6 μM, when the antibiotic is aggregated in the lipid bilayer. Below this critical concentration, the mean lifetime measured for Nystatin is considerably shorter than the typical values measured for *t*-PnA in gel phase lipids. The distinct locations in the lipid vesicles predicted for the fluorescent groups of each molecule, and thereby the different environments sensed by each one, are again the most likely justification for their different photophysical properties. At low concentrations, Nystatin must be monomeric and presumably adsorbed at the bilayer surface, whereas the fluorophore of *t*-PnA is always deeply inserted in the lipid bilayer (Castanho et al., 1995). This shallower location of Nystatin must confer a less rigid environment with a higher polarizability for its chromophore, and hence its long-lived fluorescence decay component has a smaller associated amplitude.

It is also interesting to note the absence of any spectral alteration upon Nystatin aggregation in the lipid bilayer. Because the most likely picture for the structure of a Nystatin aggregate is a stacked arrangement of antibiotic molecules with their transition dipoles parallel to each other, one would anticipate the appearance of a new blueshifted band in Nystatin absorption spectrum upon its self-association in the bilayer due to exciton coupling between the tetraene chromophores. In fact, the observation of this type of interactions has previously been used to demonstrate the close binding of the first two fluorescent fatty acids to albumin (Berde et al., 1979) and the aggregation of *t*-Pna in the lipid vesicles (Sklar et al., 1979). These spectral alterations are also very characteristic of the polyene antibiotics (Castanho et al., 1992; Balakrishnan and Easwaran, 1993a). It should be noted, however, that the physical requirements (distances and relative dipole orientations) for the exciton coupling between two neighboring chromophores are very

strict (Cantor and Schimmel, 1980). Therefore, the absence of any spectral alteration in the excitation spectrum of Nystatin at concentrations higher than 5–6 μM suggests that its chromophores are not in sufficiently close contact for an exciton interaction between their transition dipoles to be possible.

For the lipid vesicles in liquid-crystalline phase, the decay parameters of Nystatin were shown to be concentration independent (Fig. 8 *c*), suggesting that the antibiotic is monomeric within the concentration range studied. It is not possible to discriminate between a lower partition coefficient of Nystatin and the different structural characteristics displayed by the bilayer at this temperature as the main reasons for this behavior of Nystatin. Ultimately, these hypothesis are related, i.e., at this temperature the highly disordered state of the acyl chains of the phospholipids induced a decrease in the partition of the antibiotic between the aqueous and lipid phases, and therefore reduced the probability of self-association of the antibiotic in the lipid bilayer.

Relation of results to AmpB

It has usually been assumed that the molecular basis of Nystatin and AmpB action at the membrane level may be described by a single common model, although Nystatin displays an activity that is generally weaker than that of AmpB (Bolard, 1986).

Because of their amphiphilic character, these molecules readily aggregate in aqueous solution, rendering the characterization of the first steps involved in their interaction with the phospholipid bilayer membranes very difficult. CD has been extensively used in the elucidation of this problem, particularly for AmpB (Bolard et al., 1980; Vertut-Croquin et al., 1983; Jullien et al., 1988; Balakrishnan and Easwaran, 1993a), because it was shown to be a very sensitive spectroscopy capable of monitoring different antibiotic forms in the lipid bilayer. These studies demonstrated that the measurement of a specific CD spectrum for AmpB was critically dependent on several factors such as the type of the vesicle used, the physical state of the phospholipids, the antibiotic-to-lipid ratio used (*R*), the sterol content of the vesicles, and the time elapsed after sample preparation. Most importantly, for SUVs prepared with saturated phospholipids and without sterols, AmpB exhibited distinct CD spectra at low and high molar ratios of antibiotic to total lipid, which could also differ for the vesicles in gel or liquid-crystalline phases (Bolard et al., 1981; Bolard and Cheron, 1982; Jullien et al., 1988; Balakrishnan and Easwaran, 1993a). These spectra were generally interpreted as being due to monomeric antibiotic interacting with the lipid bilayer (at low *R*) and to the formation of aggregates of AmpB (at high *R*). Although a direct extrapolation of these results to Nystatin cannot be made, these data nevertheless support the conclusions of the present work.

CONCLUSIONS

Steady-state and time-resolved fluorescence measurements were used in the present work to study Nystatin interaction with a membrane model system composed of a single phospholipid (DPPC); in addition, its behavior in methanol and aqueous solution was characterized. This polyene macrolide antibiotic is intrinsically fluorescent and its tetraene fluorophore proved to be an excellent reporter of the structural organization of the antibiotic, both in homogeneous media and in lipid bilayers. In methanol, Nystatin was monomeric until a concentration of 100–200 μM was reached, whereas in aqueous solution the antibiotic was shown to aggregate with a critical concentration of 3 μM. Moreover, the steady-state fluorescence anisotropy measurements showed that Nystatin self-association in buffer followed a micellization-type equilibrium, i.e., the antibiotic formed aggregates with an approximately constant volume. The enhancement in the fluorescence intensity of Nystatin was used to assess its binding to the phospholipid vesicles and it was shown that Nystatin partitioned preferentially into gel phase lipids instead of fluid lipids, with an almost fivefold larger partition coefficient. Furthermore, a time-resolved fluorescence study was used to demonstrate Nystatin self-association in gel-phase DPPC vesicles. The antibiotic intensity-weighted mean lifetime, which was shown to be essentially controlled by the amplitude of the longest-lived decay component, displayed an abrupt transition in its value from 10 to 33 ns at an overall antibiotic concentration in solution of 5–6 μM. This observation was explained by a self-association of monomeric antibiotic molecules within the lipid bilayer; the fluorophore of Nystatin experienced a more rigid environment in the aggregates and thus its mean lifetime increased. It should be stressed that some experimental results and the main conclusions of this work contradict a previous fluorescence study of Nystatin performed by Petersen et al. (1987). Specifically, in this work no fluorescence self-quenching was observed for Nystatin; this antibiotic definitely self-associates in lipid vesicles, but the new species formed were shown to be even more fluorescent than the monomers. Moreover, the hypothesis that energy migration (dipolar mechanism) could be operative with Nystatin was completely ruled out, and accordingly, the steady-state fluorescence anisotropy measured for this antibiotic was shown to be independent of the antibiotic concentration in the lipid vesicles.

APPENDIX

The binding experiments were analyzed assuming that Nystatin distributes itself between the aqueous, N_w, and lipid, N_l, phases according to a partition equilibrium upon its interaction with phospholipid vesicles:

$$N_w \rightleftarrows N_l \tag{I.1}$$

The partition coefficient, P, that governs this equilibrium is defined by

$$P = \frac{[N]_l}{[N]_w} \tag{I.2}$$

where $[N]_l = n_l/v_l$ and $[N]_l = n_w/v_w$ are the concentrations of Nystatin in lipid and aqueous phases, respectively; v_l and v_w are the volumes of the respective phases and n_l and n_w denote the amount of Nystatin in each phase. The overall concentration of Nystatin, $[N]_t$, is given by

$$[N]_t = [N]_l \frac{v_l}{v_t} + [N]_w \frac{v_w}{v_t} \quad \text{(I.3)}$$

where v_t is the total volume of the solution.

These experiments used the increase in the quantum yield, ϕ, of Nystatin upon its interaction with the lipid vesicles to monitor the extent of the antibiotic-phospholipid vesicle association. As long as the molar absorptivities of both Nystatin species at the excitation wavelength do not differ much, Eq. I.4 holds for each antibiotic concentration studied:

$$I = x_w I_w + x_l I_l \quad \text{(I.4)}$$

In the above expression, x_i and I_i correspond to the mole fraction and the fluorescence intensity of the antibiotic in state i, respectively, where $i = w$ represents the antibiotic present in the aqueous phase and $i = l$ the antibiotic partitioned into the membrane.

As with any other spectroscopic technique, this method relies on the explicit assumption that the fractional partition of Nystatin into the phospholipid vesicles is linearly proportional to the fractional change in its quantum yield, which is directly reflected in its fluorescence intensity:

$$x_l = \frac{I - I_w}{I_l - I_w} \quad \text{(I.5)}$$

Re-expressing I_w as I_0, i.e., the fluorescence intensity of the antibiotic measured in the absence of phospholipid vesicles and I_l as I_∞, i.e., the limiting value of I measured upon increasing the lipid concentration of the solution, $[L] = n_l/v_t$ and considering $v_t \cong v_w$, Eq. I.5 can be rewritten as

$$\Delta I = \frac{\Delta I_{max}[L]}{1/(P\gamma) + [L]} \quad \text{(I.6)}$$

where γ is the molar volume of the lipid, $\Delta I = I - I_0$ and $\Delta I_{max} = I_\infty - I_0$.

Finally, for a given antibiotic concentration the previous equation can be used to fit the experimental results (ΔI versus $[L]$ data) by a nonlinear least-squares regression method to provide estimates for the unknown parameters, ΔI_{max} and P.

The authors thank Dr. E. C. Melo for the use of his HPLC instrumentation and would especially like to thank Ms. M. J. Moreno for her collaboration in these analyses. The authors also gratefully acknowledge helpful discussions with Dr. A. U. Acuña (CSIC, Madrid, Spain).

This work was supported by Junta Nacional de Investigação Científica e Tecnológica (JNICT, Portugal), programs STRDA/C/SAU/257/92 and STRDA/C/CEN/421/92.

REFERENCES

Abramson, M. B., and N. Ockman. 1973. Binding at lipid surfaces: Nystatin. *J. Colloid Interface Sci.* 43:530–538.

Balakrishnan, A. R., and K. R. K. Easwaran. 1993a. Lipid-Amphotericin B complex structure in solution: a possible first step in the aggregation process in cell membranes. *Biochemistry.* 32:4139–4144.

Balakrishnan, A. R., and K. R. K. Easwaran. 1993b. CD and NMR studies on the aggregation of Amphotericin-B in solution. *Biochim. Biophys. Acta.* 1148:269–277.

Bel'kov, M. V., and S. L. Bondarev. 1987. Luminescence and optical activity of Nystatin A_1 isomers. *Zh. Prikl. Spektrosk.* 46:314–316.

Berde, C. B., B. S. Hudson, R. S. Simoni, and L. A. Sklar. 1979. Human serum albumin. Spectroscopic studies of binding and proximity relationships for fatty acids and bilirubin. *J. Biol. Chem.* 254:391–400.

Beschiaschvili, G., and J. Seelig. 1990. Mellitin binding to mixed phosphatidylglycerol/phosphatidylcholine membranes. *Biochemistry.* 29:52–58.

Bolard, J. 1986. How do the polyene macrolide antibiotics affect the cellular membrane properties? *Biochim. Biophys. Acta.* 864:257–304.

Bolard, J., and M. Cheron. 1982. Association of the polyene antibiotic Amphotericin B with phospholipid vesicles: perturbation by temperature changes. *Can. J. Biochem.* 60:782–789.

Bolard, J., P. Legrand, F. Heitz, and B. Cybulska. 1991. One-sided action of Amphotericin B on cholesterol-containing membranes is determined by its self-association in the medium. *Biochemistry.* 30:5707–5715.

Bolard, J., M. Seigneuret, and G. Boudet. 1980. Interaction between phospholipid bilayer membranes and the polyene antibiotic Amphotericin B. Lipid state and cholesterol dependence. *Biochim. Biophys. Acta.* 599:280–293.

Bolard, J., A. Vertut-Croquin, B. Cybulska, and C. M. Gary-Bobo. 1981. Transfer of the polyene antibiotic Amphotericin B between single-walled vesicles of dipalmitoylphosphatidylcholine and egg-yolk phosphatidylcholine. *Biochim. Biophys. Acta.* 647:241–248.

Borowski, E., J. Zielinski, T. Falkowski, J. Golik, P. Kolodziejczyk, E. Jereczek, M. Gdulewicz, Y. Shenin, and T. Kotenko. 1971. The complete structure of the polyene macrolide antibiotic Nystatin A_1. *Tetrahedron Lett.* 8:685–690.

Cantor, C. R., and P. R. Schimmel. 1980. Biophysical Chemistry, Vol. II. W. H. Freeman, New York. 390–398.

Castanho, M. A. R. B., A. Coutinho, and M. J. E. Prieto. 1992. Absorption and fluorescence spectra of polyene antibiotics in the presence of cholesterol. *J. Biol. Chem.* 267:204–209.

Castanho, M., M. Prieto, and A. U. Acuña. 1995. The transverse location of the fluorescent probe *trans*-parinaric acid in lipid bilayers. *Biochim. Biophys. Acta.* In press.

De Kruijff, B., and R. A. Demel. 1974. Polyene antibiotic-sterol interactions in membranes of *Acholeplasma laidlawii* cells and lecithin liposomes. III. Molecular structure of the polyene antibiotic-cholesterol complexes. *Biochim. Biophys. Acta.* 339:57–70.

De Kruijff, B., W. J. Gerritsen, A. Oerlemans, R. A. Demel, and L. L. M. Van Deenen. 1974. Polyene antibiotic-sterol interactions in membranes of *Acholeplasma laidlawii* cells and lecithin liposomes. I. Specificity of the membrane permeability changes induced by the polyene antibiotics. *Biochim. Biophys. Acta.* 339:30–43.

Ermishkin, L. N., Kh. M. Kasumov, and V. M. Potzeluyev. 1976. Single ionic channels induced in lipid bilayers by polyene antibiotics Amphotericin B and Nystatine. *Nature.* 262:698–699.

Farinha, J. P. S., J. M. G. Martinho, H. Xu, M. A. Winnik, and R. P. Quirk. 1994. Influence of intrachain hydrogen bonding on the cyclization of a polystyrene chain. *J. Polym. Sci. [B].* 32:1635–1642.

Harkness, J. E., and R. D. White. 1979. An ultrasonic study of the thermotropic transition of dipalmitoyl phosphatidylcholine. *Biochim. Biophys. Acta.* 552:450–456.

Hartsel, S. C., S. K. Benz, R. P. Peterson, and B. S. Whyte. 1991. Potassium-selective Amphotericin B channels are predominant in vesicles regardless of sidedness. *Biochemistry.* 30:77–82.

Holz, R., and A. Finkelstein. 1970. The water and nonelectrolyte permeability induced in thin lipid membranes by the polyene antibiotics Nystatin and Amphotericin B. *J. Gen. Physiol.* 56:125–145.

HsuChen, C.-C., and D. S. Feingold. 1973. Polyene antibiotic action on lecithin liposomes: effect of cholesterol and fatty acyl chains. *Biochem. Biophys. Res. Commun.* 51:972–978.

Hudson, B., and S. A. Cavalier. 1988. Studies of membrane dynamics and lipid-protein interactions with parinaric acid. *In* Spectroscopic Membrane Probes, Vol. 1. L. M. Loew, editor. CRC Press, Boca Raton, FL. 43–62.

Hudson, B. S., D. L. Harris, R. D. Ludescher, A. Ruggiero, A. Cooney-Freed, and S. A. Cavalier. 1986. Fluorescence probe studies of proteins and membranes. *In* Applications of Fluorescence in the Biomedical Sciences. D. L. Taylor, A. S. Waggoner, F. Lanni, R. F. Murphy, and R. Birge, editors. Alan R. Liss, New York. 159–202.

Hudson, B., and B. Kholer. 1974. Linear polyene electronic structure and spectroscopy. *Annu. Rev. Phys. Chem.* 25:437–460.

James, D. R., J. R. Turnbull, B. D. Wagner, W. R. Ware, and N. O. Petersen. 1987. Distributions of fluorescence decay times for parinaric acids in phospholipid membranes. *Biochemistry.* 26:6272–6277.

Jullien, S., A. Vertut-Croquin, J. Brajtburg, and J. Bolard. 1988. Circular dichroism for the determination of Amphotericin B binding to liposomes. *Anal. Biochem.* 172:197–202.

Kelly, P. M., and K. A. Nabinger. 1985. Separation of the Filipin complex by gradient-elution high-performance liquid chromatography. *J. Antibiot.* 38:485–489.

Kinsky, S. C., S. A. Luse, and L. L. M. Van Deenen. 1966. Interaction of polyene antibiotics with natural and artificial membrane systems. *Fed. Proc. Fed. Am. Soc. Exp. Biol.* 25:1503–1510.

Kleinberg, M. E., and A. Finkelstein. 1984. Single-length and double-length channels formed by Nystatin in lipid bilayer membranes. *J. Membr. Biol.* 80:257–269.

Kobayashi, G. S., and G. Medoff. 1977. Antifungal agents: recent developments. *Annu. Rev. Microbiol.* 31:291–308.

Lackowicz, J. R. 1983. Principles of Fluorescence Spectroscopy. Plenum Press, New York.

Lambing, H. E., B. D. Wolf, and S. C. Hartsel. 1993. Temperature effects on the aggregation state and activity of Amphotericin B. *Biochim. Biophys. Acta.* 1152:185–188.

Lampert, R. A., L. A. Chewter, D. Phillips, D. V. O'Connor, A. J. Roberts, and S. R. Meech. 1983. Standards for nanosecond fluorescence decay time measurements. *Anal. Chem.* 55:68–73

Lawaczeck, R., M. Kainosho, and S. I. Chan. 1976. The formation and annealing of structural defects in lipid bilayer vesicles. *Biochim. Biophys. Acta.* 443:313–330.

Legrand, P., E. A. Romero, B. E. Cohen, and J. Bolard. 1992. Effects of aggregation and solvent on the toxicity of Amphotericin B to human erythrocytes. *Antimicrob. Agents Chemoter.* 36:2518–2522.

Lentz, B. R., B. M. Moore, and D. A. Barrow. 1979. Light-scattering effects in the measurement of membrane microviscosity with diphenylhexatriene. *Biophys. J.* 25:489–494.

Manwaring, D. G., R. W. Rickards, and B. T. Golding. 1969. The structure of the aglycone of the macrolide antibiotic Nystatin. *Tetrahedron Lett.* 60:5319–5322.

Marsh, D. 1990. Handbook of Lipid Bilayers. CRC Press, Boca Raton, FL. 135–136.

Marty, A., and A. Finkelstein. 1975. Pores formed in lipid bilayer membranes by Nystatin. Differences in its one-sided and two-sided action. *J. Gen. Physiol.* 65:515–526.

Mateo, C. R., J.-C. Brochon, M. P. Lillo, and A. U. Acuña. 1993. Lipid clustering in bilayers detected by the fluorescence kinetics and anisotropy of *trans*-parinaric acid. *Biophys. J.* 65:2237–2247.

Mateo, C. R., M. P. Lillo, J. González-Rodríguez, and A. U. Acuña. 1991. Lateral heterogeneity in human platelet plasma membrane and lipids from the time-resolved fluorescence of *trans*-parinaric acid. *Eur. Biophys. J.* 20:53–59.

Mazerski, J., J. Grzybowska, and E. Borowski. 1990. Influence of net charge on the aggregation and solubility behaviour of Amphotericin B and its derivatives in aqueous media. *Eur. Biophys. J.* 18:159–164.

McClare, C. W. F. 1971. An accurate and convenient organic phosphorus assay. *Anal. Biochem.* 39:527–530.

Mechlinski, W., and C. P. Schaffner. 1974. Separation of polyene antibiotics by high-speed liquid chromatography. *J. Chromatogr.* 99: 619–633.

Medoff, G., J. Brajtburg, G. S. Kobayashi, and J. Bolard. 1983. Antifungal agents useful in therapy of systemic fungal infections. *Annu. Rev. Pharmacol. Toxicol.* 23:303–330.

Mitrofanova, V. G., O. A. Mirgorodskaya, A. A. Derzhavets, E. R. Matveeva, Y. D. Shenin, and A. F. Morgunova. 1991. Investigation of component composition of reference samples of polyenic macrolide antibiotics by HPLC and SIEAP mass spectrometry. *Antibiot. Khimioter.* 36:9–11.

Morgan, C. G., B. Hudson, and P. K Wolber. 1980. Photochemical dimerization of parinaric acid in lipid bilayers. *Proc. Natl. Acad. Sci. USA.* 77:26–30.

Parker, C. A. 1968. Photoluminescence of Solutions. Elsevier, Amsterdam.

Petersen, N. O. 1985. Intramolecular fluorescence energy transfer in nitrobenzoxadiazole derivatives of polyene antibiotics. *Can. J. Chem.* 63: 77–85.

Petersen, N. O., R. Gratton, and E. M. Pisters. 1987. Fluorescence properties of polyene antibiotics in phospholipid bilayer membranes. *Can. J. Chem.* 65:238–244.

Petersen, N. O., and P. F. Henshaw. 1981. Separation of fluorescent impurities from Amphotericin B. *Can. J. Chem.* 59:3376–3378.

Rinnert, H., C. Thirion, G. Dupont, and J. Lematre. 1977. Structural studies on aqueous and hydroalcoholic solutions of a polyene antibiotic: Amphotericin B. *Biopolymers.* 16:2419–2427.

Ruggiero, A., and B. Hudson. 1989. Critical density fluctuations in lipid bilayers detected by fluorescence lifetime heterogeneity. *Biophys. J.* 55:1111–1124.

Sklar, L. A. 1980. The partition of *cis*-parinaric acid and *trans*-parinaric acid among aqueous, fluid lipid, and solid lipid phases. *Mol. Cell. Biochem.* 32:169–177.

Sklar, L. A., B. S. Hudson, M. Petersen, and J. Diamond. 1977a. Conjugated polyene fatty acids as fluorescent probes: spectroscopic characterisation. *Biochemistry.* 16:813–818.

Sklar, L. A., B. S. Hudson, and R. D. Simoni. 1977b. Conjugated polyene fatty acids as fluorescent probes: synthetic phospholipid membrane studies. *Biochemistry.* 16:819–828.

Sklar, L. A., B. S. Hudson, and R. D. Simoni. 1977c. Conjugated polyene fatty acids as fluorescent probes: binding to bovine serum albumin. *Biochemistry.* 16:5100–5108.

Sklar, L. A., G. P. Miljanich, and E. A. Dratz. 1979. Phospholipid lateral phase separation and the partition of *cis*-parinaric and *trans*-parinaric acid among aqueous, solid lipid, and fluid lipid phases. *Biochemistry.* 18:1707–1716.

Snyder, B., and E. Freire. 1982. Fluorescence energy transfer in two dimensions. A numeric solution for random and nonrandom distributions. *Biophys. J.* 40:137–148.

Somerharju, P., H. Brockerhoff, and K. W. A. Wirtz. 1981. A new fluorimetric method to measure protein-catalysed phospholipid transfer using 1-acyl-2-parinaroylphosphatidylcholine. *Biochim. Biophys. Acta.* 649:521–528.

Somerharju, P., P. Van Paridon, and K. W. A. Wirtz. 1983. Phosphatidylinositol transfer protein from bovine brain. Substrate specificity and membrane binding properties. *Biochim. Biophys. Acta.* 731: 186–195.

Strom, R., W. E. Blumberg, R. E. Dale, and C. Crifo. 1976. The interaction of the polyene antibiotic Lucensomycin with cholesterol in erythrocyte membranes and in model systems. III. Characterisation of spectral parameters. *Biophys. J.* 16:1297–1314.

Thomas, A. H., B. Pharm, P. Newland, and G. J. Quinlan. 1981. Identification and determination of the qualitative composition of Nystatin using thin-layer chromatography and high-performance liquid chromatography. *J. Chromatogr.* 216:367–373.

Van Hoogevest, P., and B. De Kruijff. 1978. Effect of Amphotericin B on cholesterol-containing liposomes of egg phosphatidylcholine and didocosenoylphosphatidylcholine. A refinement of the model for the formation of pores by Amphotericin B in membranes. *Biochim. Biophys. Acta.* 511:397–407.

Vertut-Croquin, A., J. Bolard, M. Chabbert, and C. Gary-Bobo. 1983. Differences in the interaction of the polyene antibiotic Amphotericin B with cholesterol- or ergosterol-containing phospholipid vesicles. A circular dichroism and permeability study. *Biochemistry.* 22: 2939–2944.

Zielinski, J., J. Golik, J. Pawlak, E. Borowski, and L. Falkowski. 1988. The structure of Nystatin A_3, a component of Nystatin complex. *J. Antibiot.* 41:1289–1291.

Zuker, M., A. G. Szabo, L. Bramall, D. T. Krajcarski, and B. Selinger. 1985. Delta function convolution method (DFCM) for fluorescence decay experiments. *Rev. Sci. Instrum.* 56:14–22.